

# Kink dynamics with oscillating forces

Thomas Le Goff<sup>1</sup>, Olivier Pierre-Louis<sup>1</sup>, and Paolo Politi<sup>2,3</sup>

<sup>1</sup> *Institut Lumière Matière, UMR5306 Université Lyon 1-CNRS, Université de Lyon 69622 Villeurbanne, France*

<sup>2</sup> *Istituto dei Sistemi Complessi, Consiglio Nazionale delle Ricerche,  
Via Madonna del Piano 10, 50019 Sesto Fiorentino, Italy*

<sup>3</sup> *INFN Sezione di Firenze, via G. Sansone 1, 50019 Sesto Fiorentino, Italy.*

(Dated: December 3, 2024)

It is well known that the dynamics of a one-dimensional dissipative system driven by the Ginzburg-Landau free energy  $\mathcal{F}_{\text{GL}}$  may be described in terms of interacting kinks with a nearest neighbors attractive force  $F(\ell) \approx \exp(-\ell)$ . This result is typical of a bistable system whose inhomogeneities have an energy cost due to surface tension, proportional to the square of the derivative of the profile ( $\int dx h_x^2$ ). There are however cases where bending rigidity ( $\int dx h_{xx}^2$ ) rather than surface tension plays a leading role. We show that a kink dynamics is still applicable, but the force  $F(\ell)$  between two kinks at distance  $\ell$  is now oscillating, therefore producing configurations which are locally stable. Our derivation of kink dynamics is general and original. It applies to a generalized Ginzburg-Landau free energy with an arbitrary combination of surface tension, bending energy, and higher-order terms. Furthermore, it is not based on a specific multikink approximation and the resulting kink dynamics reproduces correctly the true full dynamics of the original model. This allows to use our derivation with confidence in place of the continuum dynamics, reducing simulation time by four orders of magnitude.

PACS numbers: 05.45.-a, 05.70.Ln, 02.30.Jr

## I. THE CLASSICAL PICTURE OF KINK DYNAMICS

The Ginzburg-Landau free energy is an important building block to study equilibrium and nonequilibrium phenomena. Its actual expression mainly depends on the symmetry of the order parameter and on the dimensionality of the physical system. In the simplest possible scenario, a scalar order parameter in a one-dimensional system,

$$\tilde{\mathcal{F}}_{\text{GL}} = \int dx \left( \frac{K_1}{2} h_x^2 + \tilde{U}(h) \right) \quad (1)$$

where  $\tilde{U}(h)$  is an arbitrary symmetric double well potential, with two equivalent minima for  $h = \pm h_m$  which are the ground states of the full free energy. If  $\tilde{U}(h) = U_0 U(h)$ , rescaling space we get

$$\tilde{\mathcal{F}}_{\text{GL}} = \sqrt{K_1 U_0} \int dx \left( \frac{1}{2} h_x^2 + U(h) \right) \equiv e_0 \mathcal{F}_{\text{GL}}. \quad (2)$$

In the following the energy scale  $e_0$  will be set equal to one, while we don't rescale  $h_m$  to one for pedagogical reasons.

In this Section, for definiteness, we consider a standard quartic potential,  $U(h) = -h_m^2 h^2/2 + h^4/4$ , thus  $\mathcal{F}_{\text{GL}}$  has local minima connecting the two ground states of simple form, called kink (+) and antikink (-),

$$h(x) = \pm h_k(x) \equiv \pm h_m \tanh \left( \frac{h_m}{\sqrt{2}} x \right). \quad (3)$$

The physical meaning of the first term in  $\mathcal{F}_{\text{GL}}$  is easily understood if it is read as the dominant term in a Taylor expansion of the total length  $L$  of the  $h$ -profile, with respect to the slope,  $L = \int dx \sqrt{1 + h_x^2} \approx L_0 + \frac{1}{2} \int dx h_x^2$ . The standard example of physical system where such term emerges is a ferromagnet, whose exchange coupling is

$$E_{ex} = - \int dx \int dx' J(|x - x'|) m(x) m(x'). \quad (4)$$

If we rewrite

$$-2m(x)m(x') = (m(x) - m(x'))^2 - (m^2(x) + m^2(x')), \quad (5)$$

the first term on the RHS, once Taylor expanded, produces exactly the surface tension term. The second term on the right contributes instead to  $U(h)$ , along with entropic terms.

The free energy  $\mathcal{F}_{\text{GL}}$  is also the starting point to study the dissipative dynamics when the system is relaxing towards equilibrium. When studying dynamics the existence of conservation laws is of primary importance and two main universality classes exist, depending on whether the order parameter,  $\int dx h(x, t)$ , is conserved (CH) or not (TDGL):

$$\partial_t h(x, t) = - \frac{\delta \mathcal{F}_{\text{GL}}}{\delta h} = h_{xx} + h_m^2 h - h^3 \quad \text{TDGL} \quad (6)$$

$$\partial_t h(x, t) = \partial_{xx} \frac{\delta \mathcal{F}_{\text{GL}}}{\delta h} = -\partial_{xx} (h_{xx} + h_m^2 h - h^3) \quad \text{CH} \quad (7)$$

In both cases, it is straightforward to show that

$$\frac{d\mathcal{F}_{\text{GL}}}{dt} = \int dx \frac{\delta \mathcal{F}}{\delta h} \frac{\partial h}{\partial t} \leq 0. \quad (8)$$

The nonconserved Eq. (6) typically describes phase separation in a magnet, because in this case relaxation dynamics does not conserve magnetization. The equation is known by many different names: Fisher-Kolmogorov, Allen-Cahn, real Ginzburg Landau, Time Dependent Ginzburg Landau equation. We will use the last. The conserved Eq. (7) may describe phase separation in a binary alloy, where matter (the integral of density, the order parameter) is conserved. It is called Cahn-Hilliard equation.

In the above two cases, TDGL and CH equations, the overall picture of dynamics is well known. The solution  $h = 0$ , corresponding to the disordered or homogeneous phase, is linearly unstable and small regions of the two phases  $h = \pm h_m$  appear. These regions are separated by kinks, which feel an attractive interaction. When a kink and an antikink meet they annihilate, therefore leading to an increasing distance between them (coarsening process). This process lasts forever, but in one dimension it is logarithmically slow if noise is absent.

The above picture is well known and it goes back to works by Langer [1] and Kawasaki and Ohta [2]. The main idea is to write  $h(x, t)$  as a suitable superposition of positive and negative kinks, getting a set of discrete equations for their positions  $x_n(t)$ . The Partial Differential Equation (PDE) (6) or (7) determines the kink dynamics in two respects: (i) the profile of the single kink solution, and (ii) the effective interaction between kinks. In fact, the form of the interaction descends directly from the shape of the kink, as it will be shown in Sec. III. Therefore, once we specify if the dynamics is conserved or not, it is not arbitrary to state that ensuing dynamics follows from the hyperbolic tangent profile of the kink, see Eq. (3).

Even if a term proportional to  $h_x^2$  in the free energy is well justified (see above discussion), we should not come to the conclusion that surface tension always plays a dominant role. In fact, here we are interested to study how kink dynamics is affected by bending rigidity rather than by tension [3]. The introduction of this mechanism will be justified in the next Section, where we are also going to show that its main effect is to modify the kink profile, which is no more monotonous. Rather, it has an oscillating behavior around the minima of  $U(h)$ , which determines an oscillating interaction between kinks. This fact will be qualitatively understood within a unified picture where kink profile and kink interaction are directly related. Such oscillating interaction modifies phase space leading to a plethora of steady states many of which are linearly stable, therefore strongly affecting dynamics.

In general terms, we believe that a systematic derivation of kink dynamics from a continuum description of the system is not available. For this reason in Sec. IV we propose an alternative and transparent derivation, which appears to be very reliable from a quantitative point of view.

## II. THE EFFECT OF BENDING RIGIDITY

It has been simple to explain why a magnetic domain wall has a free energy term proportional to  $h_x^2$ : in that case  $h(x)$  means the local magnetization and its spatial variation costs energy because spins would like to stay parallel. The same argument may apply to a completely different context, a crystal surface where  $h(x)$  is the local height and the surface energy is proportional to the total number of broken bonds, i.e. to the total extension of the surface. A similar energy term also appears in all nucleation problems where surface and volume energies compete during the dynamics of a first order transition.

However, we may also think to *objects* whose absolute orientation is irrelevant and whose energy depends on their bending [4]. These objects are specially important in biophysics and soft matter. If bending rigidity dominates over surface tension, the Ginzburg-Landau free energy should be written

$$\mathcal{F}_{\text{GL4}} = \int dx \left[ \frac{1}{2} h_{xx}^2 + U(h) \right]. \quad (9)$$

It's quite natural to wonder how Eqs. (6,7) are modified by replacing  $\mathcal{F}_{\text{GL}}$  with  $\mathcal{F}_{\text{GL4}}$ . The answer is easily obtained and it is given by the following pair of equations,

$$\partial_t h(x, t) = -h_{xxxx} + h_m^2 h - h^3 \quad \text{TDGL4} \quad (10)$$

$$\partial_t h(x, t) = -\partial_{xx} (-h_{xxxx} + h_m^2 h - h^3) \quad \text{CH4}, \quad (11)$$

where the label '4' highlights the replacement of a second spatial derivative with a fourth spatial derivative. It is worthnoting that the change of sign of the higher order derivative is essential to ensure stability at arbitrarily small lengthscales. This is easily seen by a linear stability analysis of the solution  $h = 0$ . If  $h(x, t) = \varepsilon e^{\sigma t} e^{iqx}$ , at first order in  $\varepsilon$  we get

$$\sigma(q) = \begin{cases} h_m^2 - q^4 & \text{TDGL4} \\ h_m^2 q^2 - q^6 & \text{CH4} \end{cases}. \quad (12)$$

A positive sign of the higher order derivative in Eqs. (10,11) would have determined a positive  $\sigma(q)$  for any  $q$ , i.e. instability at *all* lengthscales, which is an unphysical picture.

The study of steady states is not straightforward as for TDGL/CH, where it essentially boils down to solve the problem of a particle of coordinate  $h$  in the potential  $V(h) = -U(h)$ . Now steady states are determined by the time independent equation

$$-h_{xxxx} - U'(h) = 0. \quad (13)$$

This fact is trivial for TDGL4, while for CH4 we must assume that  $h(x)$  is limited and of zero mean.

The fourth order derivative introduces new classes of kinks, because fixing the conditions  $h(x \rightarrow \pm\infty) = \pm 1$  is no longer sufficient to uniquely determine a solution. According to Ref. [5] kinks can be labeled by their number of zeros,

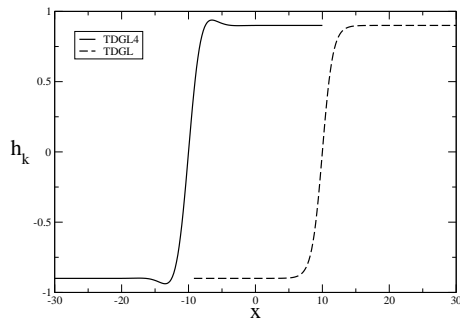


FIG. 1. Plot of kinks appearing in TDGL/CH (dashed line) and in TDGL4/CH4 (full line). In the latter case, the tail continues to oscillate around  $\pm h_m$ , but its exponential decay allows to make visible only the first two oscillations.

but their asymptotic behavior is the same because it is determined by the linearization of the above equation around  $h = h_m$ ,

$$h_{xxxx} = -U''(h_m)(h - h_m). \quad (14)$$

It is easily found that  $h(x) = h_m + R(x)$ , where the tail  $R(x)$  is given by

$$R(x) = A \cos(\kappa x + \alpha) \exp(-\kappa x), \quad (15)$$

where  $\kappa = (U''(h_m))^{1/4}/\sqrt{2}$ , while the amplitude  $A$  and the phase  $\alpha$  are undetermined within the linear theory. The exact shape of kinks for TDGL and TDGL4 models is plotted in Fig. 1, where we limit for TDGL4 to the one-zero kink.

A similar picture, oscillating kinks and kinks with more zeros, emerges in other PDEs, e.g. the convective Cahn-Hilliard equation [6]. In both cases there is no evidence of such multihump kinks during dynamics, which lead us to assume they are dynamically irrelevant. Therefore in the next Section we are studying kink dynamics assuming only one class of kinks.

### III. KINK DYNAMICS MADE SIMPLE

The main feature which differentiates the tail of Eq. (15) with respect to the ‘standard’ TDGL/CH case is the oscillating factor  $\cos(\kappa x + \alpha)$ , which makes the kink a nonmonotonous function. The following, semiquantitative treatment of a profile simply consisting of the superposition of a negative and a positive kink allows to grasp the relation between the kink tail  $R(x)$  and the kink interaction.

In order to get a result as general as possible, we consider an energy functional which is the sum of a symmetric double well potential (as before) plus an arbitrary linear, local operator satisfying the symmetry  $x \rightarrow -x$ :

$$\mathcal{F} = \int dx \left[ U(h) - \frac{1}{2} \sum_{i=0}^M (-1)^i a_{2i} (\partial_x^i h)^2 \right]. \quad (16)$$

Here above we have introduced the factor  $\frac{1}{2}(-1)^i$  so as to get rid of it when evaluating the functional derivative

$$\begin{aligned} \frac{\delta \mathcal{F}}{\delta h} &\equiv \frac{\delta}{\delta h} \int dx F(h, \partial_x h, \partial_{xx} h, \dots) \\ &= \frac{\partial F}{\partial h} + \sum_{j=1}^M (-1)^j \partial_x^j \frac{\partial F}{\partial (\partial_x^j h)} \\ &= U'(h) - \sum_{j=1}^M a_{2j} \partial_x^{2j} h \\ &\equiv U'(h) - \mathcal{L}[h] \end{aligned} \quad (17)$$

The PDE we are going to analyze is the nonconserved model driven by  $\mathcal{F}$ ,  $\partial_t h = -(\delta\mathcal{F}/\delta h)$ , i.e.,

$$\partial_t h = \mathcal{L}[h] - U'(h). \quad (18)$$

If  $h_k(x)$  is the kink profile centred at  $x = 0$ , the two-kinks approximation amounts to write

$$h(x, t) = h_k(x + x_0(t)) - h_k(x - x_0(t)) - h_m, \quad (19)$$

where the kinks are now centred in  $\pm x_0$  and dynamics preserves the symmetry  $h(-x, t) = h(x, t)$ . Within this approximation, it is easy to evaluate  $\partial_t h$ ,

$$\partial_t h(x, t) = \dot{x}_0 (h'_k(x + x_0) + h'_k(x - x_0)) \quad (20)$$

and its spatial integration,

$$\int_{-\infty}^{+\infty} dx \partial_t h(x, t) = 4h_m \dot{x}_0. \quad (21)$$

As for the RHS of Eq. (18), while we simply have  $\mathcal{L}[h] = \mathcal{L}[h_k(x + x_0)] - \mathcal{L}[h_k(x - x_0)]$ , the evaluation of  $U'(h)$  is a bit more involved. As soon as  $|x| \gg a$ ,  $a$  being the size of the core of the kink,  $h_k(x) \simeq \pm[h_m + R(|x|)]$ , for  $x \geq 0$  respectively. Therefore, we can approximate Eq. (19) as follows

$$h(x, t) \simeq \begin{cases} h_k(x + x_0) + R(-x + x_0) & x < 0 \\ -h_k(x - x_0) + R(x + x_0) & x > 0 \end{cases} \quad (22)$$

and write, in the two cases,

$$U'(h) \simeq \begin{cases} U'(h_k(x + x_0)) + U''(h_k(x + x_0))R(-x + x_0) \\ -U'(h_k(x - x_0)) + U''(h_k(x - x_0))R(x + x_0) \end{cases}, \quad (23)$$

so that

$$\begin{aligned} \int_{-\infty}^{+\infty} dx U'(h) &= \int_{-\infty}^{+\infty} dx [U'(h_k(x + x_0)) - U'(h_k(x - x_0))] \\ &+ \int_{-\infty}^0 dx [U'(h_k(x - x_0)) + U''(h_k(x + x_0))R(-x + x_0)] \\ &+ \int_0^{+\infty} dx [-U'(h_k(x + x_0)) + U''(h_k(x - x_0))R(x + x_0)]. \end{aligned} \quad (24)$$

The first line on the RHS sums up to  $\mathcal{L}[h]$  and vanish, because  $\mathcal{L}[h_k(x \pm x_0)] - U'(h_k(x \pm x_0)) = 0$ . The second and third lines give the same contribution, as a variable change  $x \rightarrow -x$  easily proves. Therefore, in conclusion we get

$$\begin{aligned} \dot{x}_0 &= \\ &\frac{1}{2h_m} \int_0^{\infty} dx [U'(h_k(x + x_0)) - U''(h_k(x - x_0))R(x + x_0)] = \\ &\frac{1}{2h_m} \int_0^{\infty} dx [U''(h_m) - U''(h_k(x - x_0))]R(x + x_0) + \mathcal{O}(R^2) \end{aligned} \quad (25)$$

The function within square brackets is vanishingly small when  $|x - x_0| \gg a$ , so we can finally write

$$\dot{x}_0 \simeq \frac{a}{2h_m} [U''(h_m) - U''(0)]R(\ell), \quad (26)$$

with  $\ell = 2x_0$ . Therefore, the speed of the right kink is barely proportional to  $R(\ell)$ , where  $\ell$  is its distance from the left kink (the quantity in square brackets being positive).

This result means that a kink exerts a force on its right neighbour at distance  $\ell$ , force which is proportional to  $R(\ell)$ , where  $R(x)$  is the difference between the kink profile and its limiting value for large, positive  $x$ ,  $R(x) = h_k(x) - h_m$ . For the standard TDGL equation,  $h_k(x) = h_m \tanh(\frac{h_m}{\sqrt{2}}x)$  and  $R(x) = R_2(x)$ , with

$$R_2(x) = -2h_m \exp(-\frac{h_m}{\sqrt{2}}x), \quad (27)$$

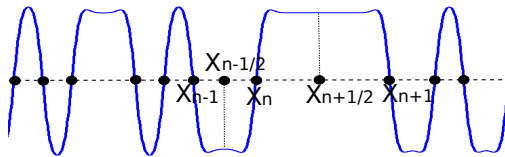


FIG. 2. (Color online) Schematic of studied system with relevant notations.

while for TDGL4,  $R(x) = R_4(x) \equiv A \cos(\kappa x + \alpha) \exp(-\kappa x)$ , see Eq. (15).

We can assume that Eq. (26) may generalize to any sequence of kinks located in  $x_n(t)$  (with  $x_{n+1} > x_n$ ) as follows,

$$\dot{x}_n = \frac{a}{2h_m} (U''(h_m) - U''(0)) [R(x_n - x_{n-1}) - R(x_{n+1} - x_n)], \quad (28)$$

with the additional constraint that two neighbouring kinks annihilate when they overlap (see details on numerical schemes in Appendix).

As a matter of fact, such kink dynamics can be derived using a superposition of  $N$  kinks,

$$\begin{aligned} h(x, t) &= (-1)^n h_k(x - x_n(t)) \\ &+ \sum_{k < n} (-1)^k [h_k(x - x_k(t)) - h_m] \\ &+ \sum_{k > n} (-1)^k [h_k(x - x_k(t)) + h_m] \end{aligned} \quad (29)$$

which is the approach used by Kawasaki and Ohta [2] to study TDGL and CH equations and by one of the authors [7] to study a conserved equation where the up-down symmetry  $h \rightarrow -h$  is broken. This approach is very reasonable and it is surely correct to have semiquantitative results. Therefore, conclusions based on such approximation [2, 7–11] and studying the coarsening process *are* correct. However, if we want to use kink dynamics in place of a direct simulation of the continuum equation, such approximation might not be satisfying, as already pointed out by Ei and Ohta [12]. This is even more true for oscillating kinks, as discussed in details in the next Section.

#### IV. IMPROVED KINK DYNAMICS

In this Section we provide a more general approach to kink dynamics, because we don't assume explicitly a specific "multikink" approximation and because we consider the general energy functional given in Eq. (16). We don't claim our approach is rigorously founded: its validity (and usefulness) are rather supported by the final comparison with numerics.

##### A. Nonconserved case

The nonconserved case corresponds to the dynamics

$$\partial_t h = -\frac{\delta \mathcal{F}}{\delta h} = \sum_i a_{2i} \partial_x^{2i} h - U'(h). \quad (30)$$

In Fig. 2 we show the schematic of the system. It has been drawn for TDGL4/CH4 kinks, but notations are generally valid. More precisely,  $x_n$  means the position of  $n$ -th kink and  $x_{n \pm \frac{1}{2}}$  the points halfway between kinks  $n$  and  $(n \pm 1)$ . For ease of notation,  $x_{n \pm \frac{1}{2}}$  is replaced by  $n \pm \frac{1}{2}$  in integrals' extrema and  $h(x_{n \pm \frac{1}{2}})$  is replaced by  $h_{n \pm \frac{1}{2}}$ .

We assume that apart from the annihilation process, which occurs when  $\ell_n = x_{n+1} - x_n \approx a$ , kinks retain their profile when moving. So, for  $x$  around  $x_n$  the previous equation can be rewritten as

$$-\dot{x}_n \partial_x h = \sum_i a_{2i} \partial_x^{2i} h - U'(h). \quad (31)$$

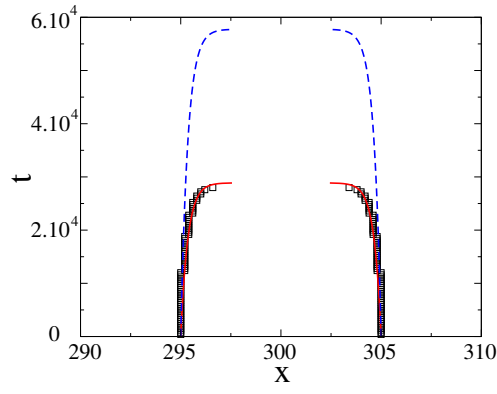


FIG. 3. (Color online) Exact dynamics and analytical approximations of the motion of two kinks for the TDGL model. Black squares: exact dynamics (integration of Eq. (6)). Red full line: our model, Eq. (38), and Ei and Ohta's model. Blue dashed line: Kawasaki and Ohta's model. In the latter model kink speeds are half than in our model, therefore dashed line corresponds to double the time of the full line.

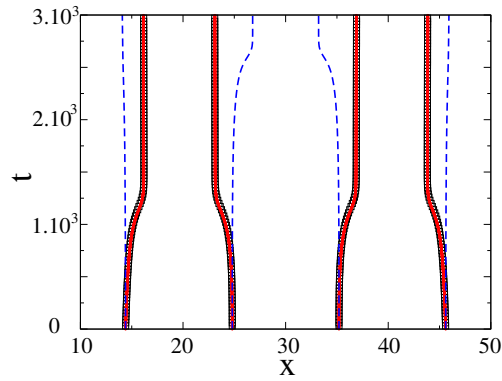


FIG. 4. (Color online) Exact dynamics and analytical approximations of the motion of four kinks for the TDGL4 model. Black squares: exact dynamics (integration of Eq. (10)). Red full line: our model, Eq. (41). Blue dashed line: Kawasaki and Ohta's model. Now, latter model can no more be rescaled to our model.

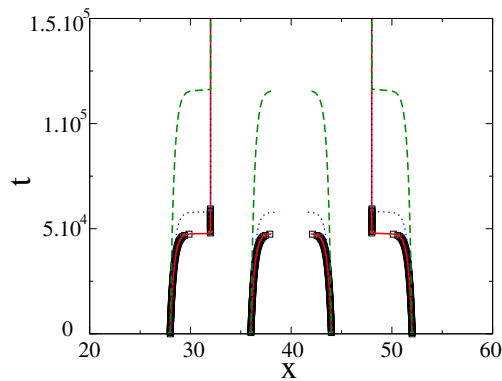


FIG. 5. (Color online)

Exact dynamics and analytical approximations of the motion of four kinks for the CH model. Black squares: exact dynamics (integration of Eq. (7)). Red full line: our model, Eq. (46). Blue dotted line: our model without the terms in  $\dot{x}_{n\pm 1}$ . Green dashed line: Kawasaki and Ohta's model.

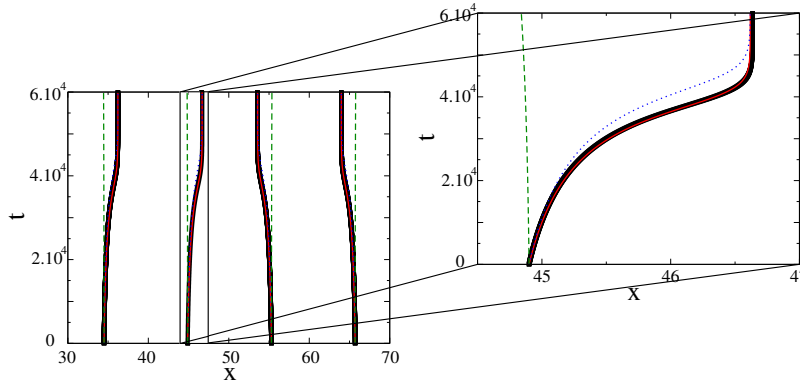


FIG. 6. (Color online) Exact dynamics and analytical approximations of the motion of four kinks for the CH4 model. Black squares: exact dynamics (integration of Eq. (11)). Red full line: our model, Eq. (47). Blue dotted line: our model without the terms in  $\dot{x}_{n\pm 1}$ . Green dashed line: Kawasaki and Ohta's model.

We then multiply both terms by  $\partial_x h$  and integrate between  $x_{n-\frac{1}{2}}$  and  $x_{n+\frac{1}{2}}$  :

$$-\dot{x}_n \int_{n-\frac{1}{2}}^{n+\frac{1}{2}} dx (\partial_x h)^2 = \sum_i a_{2i} \int_{n-\frac{1}{2}}^{n+\frac{1}{2}} dx \partial_x h \partial_x^{2i} h - U(h_{n+\frac{1}{2}}) + U(h_{n-\frac{1}{2}}).$$

Direct integration and integration by parts give

$$\dot{x}_n = \frac{1}{\int_{n-\frac{1}{2}}^{n+\frac{1}{2}} dx (\partial_x h)^2} \left[ \sum_i a_{2i} \left( \frac{(-1)^i}{2} [(\partial_x h)^2]_{n-\frac{1}{2}}^{n+\frac{1}{2}} + \sum_{k=1}^{k < \frac{i}{2}} [\partial_x^{2k} h \partial_x^{2i-2k} h]_{n-\frac{1}{2}}^{n+\frac{1}{2}} \right) + U(h_{n+\frac{1}{2}}) - U(h_{n-\frac{1}{2}}) \right]. \quad (32)$$

We stress that above result derives from one single assumption,  $\partial_t h \simeq -\dot{x}_n \partial_x h$  for  $x$  close to  $x_n$ . Equation (32) can be further elaborated because in the region halfway between  $x_n$  and  $x_{n+1}$  we can expand  $h(x, t)$  around the asymptotic values  $\pm h_m$ ,

$$h(x, t) \simeq \pm [h_m + R(x - x_n) + R(x_{n+1} - x)], \quad (33)$$

where  $+/-$  applies for a positive/negative  $n$ -th kink. Using this notation, we finally get

$$\dot{x}_n = \frac{1}{\int_{-\infty}^{+\infty} dx (\partial_x h_k)^2} \left\{ \sum_i a_{2i} \left[ (1 + (-1)^i) \left( R^{(i)} \left( \frac{\ell_n}{2} \right)^2 - R^{(i)} \left( \frac{\ell_{n-1}}{2} \right)^2 \right) - 4 \sum_{k=1}^{k < \frac{i}{2}} \left( R^{(2k)} \left( \frac{\ell_n}{2} \right) R^{(2i-2k)} \left( \frac{\ell_n}{2} \right) - R^{(2k)} \left( \frac{\ell_{n-1}}{2} \right) R^{(2i-2k)} \left( \frac{\ell_{n-1}}{2} \right) \right) \right] + 2U''(h_m) \left( R^2 \left( \frac{\ell_n}{2} \right) - R^2 \left( \frac{\ell_{n-1}}{2} \right) \right) \right\}, \quad (34)$$

where, at denominator of Eq. (32), we made the approximation

$$\int_{n-\frac{1}{2}}^{n+\frac{1}{2}} dx (\partial_x h)^2 \simeq \int_{n-\frac{1}{2}}^{n+\frac{1}{2}} dx (\partial_x h_k)^2 \simeq \int_{-\infty}^{+\infty} dx (\partial_x h_k)^2, \quad (35)$$

i.e., we have assumed that close to  $x_n$  the kink profile is similar to the static profile  $h_k(x)$  and we have extended the extrema of the integral to  $\pm\infty$ .

Therefore, in the general case of an equation with several terms  $a_{2i} \neq 0$  the expression of the speed of a kink is fairly complicated. One remark is in order: the different contributions to the RHS of Eq. (34) are not proportional to  $R(\ell_n)$  and  $R(\ell_{n-1})$ , as appearing in the simple approach given in the previous Section. This point is better clarified by focusing on two explicit cases.

For TDGL, the only nonvanishing term in the summation (30) is  $a_2 = 1$ , so Eq. (34) strongly simplifies to

$$\dot{x}_n = \frac{2U''(h_m)}{\int_{-\infty}^{+\infty} dx (\partial_x h_k)^2} \left[ R^2 \left( \frac{\ell_n}{2} \right) - R^2 \left( \frac{\ell_{n-1}}{2} \right) \right], \quad (36)$$

which should be compared to Eq. (48), where the two terms in square brackets here above are replaced by  $[R(\ell_n) - R(\ell_{n-1})]$ . In the specific TDGL case  $R(\ell)$  is a simple exponential, so, apart from the prefactor

$$R(\ell) = R^2 \left( \frac{\ell}{2} \right). \quad (37)$$

Therefore, for TDGL the result (34) differs from previous approaches for the prefactor only, i.e. for the time scale. Using the explicit expression  $U(h) = -\frac{h^2}{2} + \frac{h^4}{4}$ , we get

$$\dot{x}_n = 12\sqrt{2} \left[ \exp(-\sqrt{2}\ell_n) - \exp(-\sqrt{2}\ell_{n-1}) \right], \quad (38)$$

which agrees with Ei and Ohta [12] and with Carr and Pego [13]. We can now compare in Fig. 3 our result (38) with exact kink dynamics and the classical result by Kawasaki and Ohta.

Let us now show that things are different for TDGL4 equation. In this case we have only the term  $i = 2$ , with  $a_4 = -1$ , and

$$\dot{x}_n = \frac{2}{\int_{-\infty}^{+\infty} dx (\partial_x h_k)^2} \left\{ - \left[ \left( R'' \left( \frac{\ell_n}{2} \right) \right)^2 - \left( R'' \left( \frac{\ell_{n-1}}{2} \right) \right)^2 \right] + U''(h_m) \left[ R^2 \left( \frac{\ell_n}{2} \right) - R^2 \left( \frac{\ell_{n-1}}{2} \right) \right] \right\} \quad (39)$$

Now, see Eq. (15),  $R(\ell) = A \cos(\kappa\ell + \alpha) \exp(-\kappa\ell)$ , so that (even up to a constant)

$$R(\ell) \neq R^2 \left( \frac{\ell}{2} \right) \quad \text{and} \quad R(\ell) \neq R''^2 \left( \frac{\ell}{2} \right). \quad (40)$$

If we use the correct expression for  $R(\ell)$  we get

$$\dot{x}_n = \frac{2U''_m A^2}{\int_{-\infty}^{+\infty} dx (\partial_x h_k)^2} [\cos(\kappa\ell_n + 2\alpha) \exp(-\omega\ell_n) - \cos(\kappa\ell_{n-1} + 2\alpha) \exp(-\kappa\ell_{n-1})]. \quad (41)$$

In Fig. 4 we compare our results (41) with exact dynamics and former results obtained with the multikink approximation.

## B. Conserved case

Similarly to the nonconserved case, we are going to consider the general model

$$\partial_t h = -\partial_{xx} \left( \sum_i a_{2i} \partial_x^{2i} h - U'(h) \right), \quad (42)$$

which requires more involved mathematics, whose details are partly given in the Appendix. Here we provide the final result,

$$\dot{x}_n = \frac{1}{4h_m^2 \ell_n \ell_{n-1} - A_n (\ell_n + \ell_{n-1})} \{ \ell_{n-1} [\dot{x}_{n+1} A_{n+1} + f(\ell_{n+1}, \ell_{n-1})] + \ell_n [\dot{x}_{n-1} A_{n-1} + f(\ell_n, \ell_{n-2})] \} \quad (43)$$

where

$$A_n = \int_{n-\frac{1}{2}}^{n+\frac{1}{2}} dx \partial_x h \int_{n-\frac{1}{2}}^x dx' (h - h_{n-\frac{1}{2}}) \quad (44)$$

and

$$f(x, y) = \sum_i a_{2i} \left[ (1 + (-1)^i) \left( R^{(i)} \left( \frac{x}{2} \right)^2 - R^{(i)} \left( \frac{y}{2} \right)^2 \right) - 4 \sum_{k=1}^{k < \frac{i}{2}} \left( R^{(2k)} \left( \frac{x}{2} \right) R^{(2i-2k)} \left( \frac{x}{2} \right) - R^{(2k)} \left( \frac{y}{2} \right) R^{(2i-2k)} \left( \frac{y}{2} \right) \right) \right] + 2U_m'' \left( R^2 \left( \frac{x}{2} \right) - R^2 \left( \frac{y}{2} \right) \right), \quad (45)$$

which reduces to

$$\dot{x}_n = \frac{1}{4h_m^2 \ell_n \ell_{n-1} - 2\sqrt{2}(\ell_n + \ell_{n-1})} \left\{ \ell_{n-1} \left[ 2\sqrt{2}\dot{x}_{n+1} + 8U_m'' \left( \exp(-\sqrt{2}\ell_{n+1}) - \exp(-\sqrt{2}\ell_{n-1}) \right) \right] + \ell_n \left[ 2\sqrt{2}\dot{x}_{n-1} + 8U_m'' \left( \exp(-\sqrt{2}\ell_n) - \exp(-\sqrt{2}\ell_{n-2}) \right) \right] \right\} \quad (46)$$

for the CH equation, and to

$$\dot{x}_n = \frac{1}{4h_m^2 \ell_n \ell_{n-1} - A(\ell_n + \ell_{n-1})} \times \left\{ \ell_{n-1} \left[ \dot{x}_{n+1} A + 2U_m'' A^2 \left( \cos(\kappa \ell_{n+1} + 2\alpha) \exp(-\kappa \ell_{n+1}) - \cos(\kappa \ell_{n-1} + 2\alpha) \exp(-\kappa \ell_{n-1}) \right) \right] + \ell_n \left[ \dot{x}_{n-1} A + 2U_m'' A^2 \left( \cos(\kappa \ell_n + 2\alpha) \exp(-\kappa \ell_n) - \cos(\kappa \ell_{n-2} + 2\alpha) \exp(-\kappa \ell_{n-2}) \right) \right] \right\}, \quad (47)$$

for the CH4 equation, with  $A = \int_{-\infty}^{+\infty} dx (h_m^2 - h_k^2)$ .

In Figures 5 and 6 we compare, respectively, Eqs. (46,47) with exact dynamics, multikink approximations, and simplified versions of the same Eqs. (46,47).

## V. STABILITY OF STEADY STATES

In Sec. III we have shown that TDGL-kinks feel an attractive interaction while TDGL4-kinks feel an oscillating interaction, even if in both cases  $R(x)$  vanishes exponentially at large  $x$ . This fact implies two important differences, which are firstly stated, then proved: (i) all TDGL steady configurations are uniform,  $x_{n+1} - x_n = \ell$ , while TDGL4 ones may be even disordered; (ii) all TDGL steady states are unstable, while even uniform TDGL4 steady states may be unstable.

Let us rewrite Eq. (28) incorporating the positive prefactor at RHS in  $t$ ,

$$\dot{x}_n = R(x_n - x_{n-1}) - R(x_{n+1} - x_n), \quad (48)$$

whose time independent solution is  $R(\ell_n) = R(\ell_{n-1})$ , i.e.  $R(\ell_n) = r$ , with  $\ell_n = x_{n+1} - x_n$ . For the standard TDGL model  $R(x)$  is a monotonous function, so the equation  $R(\ell_n) = r$  has at most one solution. In practice, every uniform configuration  $\ell_n = \ell$  is stationary. Instead, for the TDGL4 model, the equation  $R(\ell_n) = r$  may have more than one solution, e.g.,  $\ell_n = \ell_{s1}$  and  $\ell_n = \ell_{s2}$ . Therefore, any sequence of kinks where  $\ell_n$  is either  $\ell_{s1}$  or  $\ell_{s2}$  (including random sequences) is a steady state. As for their stability, let us focus on uniform configurations and write  $\ell_n(t) = \ell + \epsilon_n(t)$ , which gives

$$\dot{\ell}_n = 2R(\ell_n) - R(\ell_{n+1}) - R(\ell_{n-1}) \quad (49)$$

$$= R'(\ell)[2\epsilon_n - \epsilon_{n+1} - \epsilon_{n-1}], \quad (50)$$

whose single harmonic solution is  $\epsilon_n(t) = \exp(\omega t + iqn)$ , with

$$\omega(q) = 4R'(\ell) \sin^2 \left( \frac{q}{2} \right). \quad (51)$$

We have stability (instability) if  $R'(\ell) < 0 (> 0)$ . Since  $R_2(x)$  is an increasing function, see Eq. (27), any uniform configuration is unstable for TDGL, a well know result which leads to a perpetual coarsening dynamics. Instead, since  $R_4(x)$  is oscillating also its derivative is oscillating and with varying  $\ell$  we get stable steady states and unstable steady states.

In the general case of a nonuniform steady state,

$$\ell_n(t) = \ell_n^* + \epsilon_n(t) \quad \text{with} \quad R(\ell_n^*) = r, \quad (52)$$

Eq. (49), which is still valid, gives

$$\dot{\epsilon}_n = 2R'(\ell_n^*)\epsilon_n - R'(\ell_{n-1}^*)\epsilon_{n-1} - R'(\ell_{n+1}^*)\epsilon_{n+1}. \quad (53)$$

The linear character of the equations allows to write  $\epsilon_n(t) = e^{\sigma t} A_n$ , getting

$$2R'(\ell_n^*)A_n - R'(\ell_{n-1}^*)A_{n-1} - R'(\ell_{n+1}^*)A_{n+1} = \sigma A_n \quad (54)$$

but the  $n$ -dependence of  $R'(\ell_n^*)$  prevents the diagonalization with Fourier modes ( $A_n \neq e^{iqn}$ ).

Multiplying Eq.(54) with  $R'(\ell_n^*)A_n^\dagger$ , summing over all  $n$ , and after some simple recombinations of the l.h.s., we obtain

$$\sum_{n=1}^N |R'(\ell_{n+1}^*)A_{n+1} - R'(\ell_n^*)A_n|^2 = \sigma \sum_{n=1}^N R'(\ell_n^*)|A_n|^2, \quad (55)$$

which shows that eigenvalues  $\sigma$  are real. Furthermore, if all quantities  $R'(\ell_n^*)$  have the same sign,  $\sigma$  has the sign of  $R'(\ell_n^*)$ . In particular, any steady-state kink configuration with  $R'(\ell_n^*) = r < 0$  for all  $n$  is stable. As a consequence, there is an infinite number of metastable configurations in which the system can be trapped and stuck during the dynamics.

If the quantities  $R'(\ell_n^*)$  exhibit both positive and negative signs, Eq. (55) does not allow to draw conclusions. However, in the simple cases of a period-2 configuration,  $\ell_n^* = \ell_{n+2}^*$ , or a period-3 configuration,  $\ell_n^* = \ell_{n+3}^*$ , we can prove that  $R'(\ell_n^*) < 0$  is also a necessary condition for stability. Let's show it explicitly for the period-2 configuration. If

$$\ell_{2n}^* = \ell_{s2} \quad \ell_{2n+1}^* = \ell_{s1}, \quad (56)$$

we get two coupled equations which are solved assuming

$$A_{2n} = c_2 e^{i2nq} \quad A_{2n+1} = c_1 e^{i(2n+1)q}. \quad (57)$$

The resulting eigenvalue equation is

$$\sigma^2 - 2(R'(\ell_{s1}^*) + R'(\ell_{s2}^*))\sigma + 4R'(\ell_{s1}^*)R'(\ell_{s2}^*)\sin^2 q = 0 \quad (58)$$

We have stability if both eigenvalues are negative, i.e.

$$\text{stability} \Leftrightarrow R'(\ell_{s1}^*) < 0 \text{ and } R'(\ell_{s2}^*) < 0. \quad (59)$$

## VI. SUMMARY AND DISCUSSION

Our paper studies kink dynamics deriving from a generalized Ginzburg-Landau free energy, see Eq. (16). The potential part of the free energy,  $U(h)$ , is the classical, symmetric double well potential, typical of a bistable system. The ‘‘kinetic’’ part of the free energy is the sum of squares of order parameter derivatives of general order.

The main motivation to study such free energy is that there are systems whose ‘‘kinetic’’ free energy is not given by surface tension, proportional to  $(h_x^2)$ , but rather to bending energy, which is proportional to  $(h_{xx}^2)$ . Since the two terms are not mutually exclusive, it is quite reasonable to consider the free energy

$$\mathcal{F} = \int dx \left[ U(h) + \frac{K_1}{2}(\partial_x h)^2 + \frac{K_2}{2}(\partial_x^2 h)^2 \right]. \quad (60)$$

Then, we have generalized previous expression to Eq. (16). However, even if our treatment is valid for general  $a_i$ , we focus on two cases:  $K_1 = a_2 = 1, K_2 = a_4 = 0$  and  $K_1 = a_2 = 0, K_2 = -a_4 = 1$ , i.e. to pure surface tension systems (to check existing results) and to pure bending systems (novel system of specific biophysical interest [3]).

Once  $\mathcal{F}$  is given, we may derive a generalized Ginzburg-Landau equation, see Eq. (30), or a generalized Cahn-Hilliard equation, see Eq. (42). The standard approach to derive an effective kink dynamics is to assume a specific form of  $h(x, t)$  as a suitable superposition of kinks,  $h_k(x - x_n(t))$ , located in  $x_n(t)$ . This method has proved to be fruitful, explaining the coarsening dynamics of TDGL/CH models [2, 8–11] and the effect of a symmetry breaking term [7]. However, from a quantitative point of view the validity of the initial approach was already questioned by Ei and Ohta [12]. A quantitative failing is even more transparent when considering the bending energy. In Figures 3-6

we make a detailed comparison of exact results (squares, derived from the direct integration of the equation) with the standard multikink approximation (dashed lines) and with our new results (full lines).

We can still ask why we should derive an approximate kink dynamics if we have the full exact dynamics of order parameter  $h(x, t)$ . There are several good reasons: (i) an analytical approach to nonlinear full dynamics is hard if not impossible; (ii) kink dynamics is easy to understand and analytical methods are feasible; (iii) numerical simulation of kink dynamics is far faster than the simulation of the full PDE.

Our derivation of kink dynamics is different from previous derivations based on the substitution of a multi-kink ansatz in the full equation. Our two assumptions are that kinks retain their profile when moving and that kink motion is so slow that the profile away from the kinks is well approximated by steady-state solutions. We do not claim that our approach is intrinsically more rigorous than others, but it appears to be quantitatively reliable for all models we have studied, as shown in Figs. 3-6.

In addition to be numerically reliable, some of our kink models (TDGL4/CH4) have the intrinsic interest to display an oscillating tail  $R(x) = h_k(x) - h_m$ . This is the reason for two important features. Firstly, an oscillating tail means an oscillating force between kinks, as opposed to the classical TDGL/CH models. Therefore, the long term dynamical scenario is not a coarsening scenario, but the freezing in one of the many metastable states. This can give rise to a consistency problem when we use the approximation  $\ell_n \gg a$  to derive kink dynamics. However, the approximation is expected to give reasonable results even for not so far kinks and comparison with exact numerics supports such claim.

Secondly, an oscillating tail  $R(x)$  is the origin of the quantitative discrepancy between classical multikink approaches and our approach, which is more correct. For example, classical results for TDGL4 provide an interkink force proportional to  $R(\ell)$  while a force  $F(\ell) \approx R^2(\ell/2)$  appears to be more appropriate. If it were  $R(\ell) \simeq \exp(-\kappa\ell)$ , the two approaches would be equivalent, apart a rescaling of time. Instead, if  $R(\ell) \simeq \cos(\kappa\ell + \alpha) \exp(-\kappa\ell)$  the two approaches are definitely different.

In this paper we have focused on the derivation of kink dynamics and on the quantitative comparison with the exact dynamics of the PDE. The kink models for TDGL4 and CH4 are also considered in Ref. [14] where we specially use them for long time dynamics of the deterministic model and for any time dynamics of the stochastic models. In fact, once we have proven (here) their quantitative reliability, we can use them with confidence whenever the direct numerical integration of PDEs would be too demanding in terms of CPU time. This is certainly the case if we require to go to very long times or if we need to add stochastic noise to the equations. Our evaluation of the simulation times for the PDE ( $t_{\text{PDE}}$ ) and for the kink model ( $t_k$ ) allows to conclude that we gain four orders of magnitude,  $t_{\text{PDE}}/t_k \approx 10^4$ .

## ACKNOWLEDGMENTS

We wish to thank Xavier Lamy for useful insights about the stability analysis of kink arrays. We also acknowledge support from Biolub Grant No. ANR-12-BS04-0008.

## Appendix A: Derivation of Eq. (43)

Let us rewrite Eq. (42),

$$\partial_t h = -\partial_{xx} \left( \sum_i a_{2i} \partial_x^{2i} h - U'(h) \right) \quad (\text{A1})$$

and we still suppose we can write  $\partial_t h \simeq -\dot{x}_n \partial_x h$ . If we integer (A1) twice between  $x_{n-\frac{1}{2}}$  and  $x$  we obtain

$$-\dot{x}_n \int_{n-\frac{1}{2}}^x dx' (h - h_{n-\frac{1}{2}}) = -\sum_i a_{2i} \partial_x^{2i} h + U'(h) + j_{n-\frac{1}{2}}(x - x_{n-\frac{1}{2}}) + \mu_{n-\frac{1}{2}},$$

with  $j = \partial_x (\sum_i a_{2i} \partial_x^{2i} h - U'(h))$  and  $\mu = \sum_i a_{2i} \partial_x^{2i} h - U'(h)$ . Then we multiply by  $\partial_x h$  and we integer between  $x_{n-\frac{1}{2}}$  and  $x_{n+\frac{1}{2}}$ :

$$-\dot{x}_n A_n = \left[ -\sum_i a_{2i} \left( \frac{(-1)^{i-1}}{2} (\partial_x^i h)^2 - \sum_{k=1}^{k < \frac{i}{2}} \partial_x^{2k} h \partial_x^{2i-2k} h \right) + U(h) \right]_{n-\frac{1}{2}}^{n+\frac{1}{2}} + j_{n-\frac{1}{2}} B_n + \mu_{n-\frac{1}{2}} [h]_{n-\frac{1}{2}}^{n+\frac{1}{2}}. \quad (\text{A2})$$

where  $A_n = \int_{n-\frac{1}{2}}^{n+\frac{1}{2}} dx \partial_x h \int_{n-\frac{1}{2}}^x dx' (h - h_{n-\frac{1}{2}})$  and  $B_n = \int_{n-\frac{1}{2}}^{n+\frac{1}{2}} dx \partial_x h (x - x_{n-\frac{1}{2}})$ .

If we do the same thing but between  $x$  and  $x_{n+\frac{1}{2}}$  we obtain :

$$-\dot{x}_n A_n = \left[ -\sum_i a_{2i} \left( \frac{(-1)^{i-1}}{2} (\partial_x^i h)^2 - \sum_{k=1}^{k < \frac{i}{2}} \partial_x^{2k} h \partial_x^{2i-2k} h \right) + U(h) \right]_{n-\frac{1}{2}}^{n+\frac{1}{2}} + j_{n+\frac{1}{2}} B'_n + \mu_{n+\frac{1}{2}} [h]_{n-\frac{1}{2}}^{n+\frac{1}{2}}, \quad (\text{A3})$$

where  $B'_n = -\int_{n-\frac{1}{2}}^{n+\frac{1}{2}} dx \partial_x h (x_{n+\frac{1}{2}} - x)$ . By summing Eq. (A2) for the  $n$ -th kink and Eq. (A3) for the  $(n-1)$ -th kink we get

$$-\dot{x}_n A_n - \dot{x}_{n-1} A_{n-1} = \left[ -\sum_i a_{2i} \left( \frac{(-1)^{i-1}}{2} (\partial_x^i h)^2 - \sum_{k=1}^{k < \frac{i}{2}} \partial_x^{2k} h \partial_x^{2i-2k} h \right) + U(h) \right]_{n-\frac{3}{2}}^{n+\frac{1}{2}} + j_{n-\frac{1}{2}} (B_n + B'_{n-1}) + \mu_{n-\frac{1}{2}} [h]_{n-\frac{3}{2}}^{n+\frac{1}{2}}. \quad (\text{A4})$$

Because of the definition of  $j$ ,  $\dot{x}_n [h]_{n-\frac{1}{2}}^{n+\frac{1}{2}} = j_{n+\frac{1}{2}} - j_{n-\frac{1}{2}}$ . Finding  $j_{n-\frac{1}{2}}$  from (A4) and  $j_{n+\frac{1}{2}}$  from the same equation with  $n \rightarrow n+1$ , we finally obtain the kink dynamics

$$\begin{aligned} \dot{x}_n [h]_{n-\frac{1}{2}}^{n+\frac{1}{2}} &= \frac{1}{B_{n+1} + B'_n} \times \\ &\left( -\dot{x}_n A_n - \dot{x}_{n+1} A_{n+1} + \left[ \sum_i a_{2i} \left( \frac{(-1)^{i-1}}{2} (\partial_x^i h)^2 - \sum_{k=1}^{k < \frac{i}{2}} \partial_x^{2k} h \partial_x^{2i-2k} h \right) - U(h) \right]_{n-\frac{1}{2}}^{n+\frac{3}{2}} - \mu_{n+\frac{1}{2}} [h]_{n-\frac{1}{2}}^{n+\frac{3}{2}} \right) \\ &- \frac{1}{B_n + B'_{n-1}} \times \\ &\left( -\dot{x}_{n-1} A_{n-1} - \dot{x}_n A_n + \left[ \sum_i a_{2i} \left( \frac{(-1)^{i-1}}{2} (\partial_x^i h)^2 - \sum_{k=1}^{k < \frac{i}{2}} \partial_x^{2k} h \partial_x^{2i-2k} h \right) - U(h) \right]_{n-\frac{3}{2}}^{n+\frac{1}{2}} - \mu_{n-\frac{1}{2}} [h]_{n-\frac{3}{2}}^{n+\frac{1}{2}} \right). \end{aligned} \quad (\text{A5})$$

We now establish the relations

$$\begin{aligned} [h]_{n-\frac{1}{2}}^{n+\frac{1}{2}} &= (-1)^n 2h_m \\ B_{n+1} + B'_n &= \int_{n+\frac{1}{2}}^{n+\frac{3}{2}} dx \partial_x h (x - x_{n+\frac{1}{2}}) - \int_{n-\frac{1}{2}}^{n+\frac{1}{2}} dx \partial_x h (x_{n+\frac{1}{2}} - x) \\ &= \int_{n+\frac{1}{2}}^{n+\frac{3}{2}} dx h_{n+\frac{3}{2}} + \int_{n-\frac{1}{2}}^{n+\frac{1}{2}} dx h_{n-\frac{1}{2}} - \int_{n-\frac{1}{2}}^{n+\frac{3}{2}} dx h \\ &\simeq (-1)^{n+1} 2h_m (x_{n+1} - x_n). \end{aligned}$$

Then, reminding that  $\mu_{n+\frac{1}{2}} = \sum_i a_{2i} \partial_x^{2i} h |_{n+\frac{1}{2}} - U'(h_{n+\frac{1}{2}})$  is very small for a membrane near the equilibrium and  $[h]_{n-\frac{1}{2}}^{n+\frac{3}{2}}$  is very small in the limit of distant kinks, Eq. (A5) becomes

$$\begin{aligned} \dot{x}_n &= \frac{-1}{4h_m^2} \left\{ \frac{1}{x_{n+1} - x_n} \left( -\dot{x}_n A_n - \dot{x}_{n+1} A_{n+1} + \left[ \sum_i a_{2i} \left( \frac{(-1)^{i-1}}{2} (\partial_x^i h)^2 - \sum_{k=1}^{k < \frac{i}{2}} \partial_x^{2k} h \partial_x^{2i-2k} h \right) - U(h) \right]_{n-\frac{1}{2}}^{n+\frac{3}{2}} \right) \right. \\ &\left. + \frac{1}{x_n - x_{n-1}} \left( -\dot{x}_{n-1} A_{n-1} - \dot{x}_n A_n + \left[ \sum_i a_{2i} \left( \frac{(-1)^{i-1}}{2} (\partial_x^i h)^2 - \sum_{k=1}^{k < \frac{i}{2}} \partial_x^{2k} h \partial_x^{2i-2k} h \right) - U(h) \right]_{n-\frac{3}{2}}^{n+\frac{1}{2}} \right) \right\} \end{aligned} \quad (\text{A6})$$

or, collecting  $\dot{x}_n$  terms in the right-hand side,

$$\dot{x}_n = \frac{1}{4h_m^2 \ell_n \ell_{n-1} - A_n(\ell_n + \ell_{n-1})} \{ \ell_{n-1} [\dot{x}_{n+1} A_{n+1} + f(\ell_{n+1}, \ell_{n-1})] + \ell_n [\dot{x}_{n-1} A_{n-1} + f(\ell_n, \ell_{n-2})] \} \quad (43)$$

where  $A_n$  and  $f(x, y)$  are defined in the main text respectively Eqs. (44) and (45).

## Appendix B: Numerical schemes

We integrate the full dynamics of various PDE's on a one-dimensional lattice with periodic boundary conditions. Space-derivatives are calculated using a finite-size difference scheme with discretization  $dx = 0.2$ . The time integration is performed using an explicit Euler scheme. The time-step depends on the equation to be solved. The most stringent case is CH6, where must be  $dt = 10^{-6}$ . Therefore, we have used this value of  $dt$  for all simulations.

Initial conditions are built from stationary kink profiles, which are known analytically for TDGL and CH. For the fourth order case, TDGL4 and CH4, these kink profiles are obtained numerically from steady-state solutions with isolated kinks. To build a kink-antikink pair at  $x_1$  and  $x_2$ , we use the profile of the stationary kink  $h_k(x - x_1)$  for  $0 \leq x \leq (x_1 + x_2)/2$ , and the profile of the stationary antikink,  $-h_k(x - x_2)$ , otherwise.

For the implementation of kink dynamics we also use an explicit Euler scheme with  $dt = 10^{-2}$ . The main difficulty comes from the annihilation of a kink-antikink pairs. Indeed, since kink models are designed to be quantitatively accurate at long inter-kink distances only, they are not necessarily accurate, or even well defined at short distances. However, kinks and antikinks merge and annihilate rapidly in the full dynamics when their separation is smaller than the size of the kink core. We therefore generically use a cutoff inter-kink distance  $a$  below which kinks and anti-kinks spontaneously annihilate in kink dynamics, using the following procedure. If the separation between the  $n$ -th and  $(n + 1)$ -th kinks is smaller than  $a$  at time  $t + dt$ , we define the collision time-step  $dt_{\text{ann}} = (x_{n+1}(t) - x_n(t)) / (\dot{x}_n(t) - \dot{x}_{n+1}(t))$  from a simple linear extrapolation. We then integrate the dynamics of all kinks up to  $t + dt_{\text{ann}}$ , and erase the two kinks at  $x_n$  and  $x_{n+1}$ .

In the non-conserved case, the full dynamics is not much affected by the choice of the cutoff, and we chose  $a = 0$  is the simulations presented in the main text. In the conserved case, the denominator  $(4h_m^2 \ell_n \ell_{n-1} - A(\ell_n + \ell_{n-1}))$  in Eq.(47) vanishes for positive  $\ell_n$  and  $\ell_{n-1}$ . Assuming that  $\ell_n \sim \ell_{n-1}$  just before the collision, we find that the critical value of the interkink distance to keep the dynamics well defined is  $\ell_c = 2/(2h_m)^2$ . Using the quartic potential  $U = -h_m^2 h^2/2 + h^4/4$ , with  $h_m = 0.9$ , we find  $A \approx 1.86$ , leading to  $\ell_c \approx 1.15$ . We find that our numerical scheme is stable for  $a \geq 1.3$ , which is consistent with the expected constraint  $a > \ell_c$ . In order to ensure strong stability, we have performed most simulations with a slightly larger value of  $a = 1.5$ .

- 
- [1] J. Langer, *Annals of Physics* **65**, 53 (1971).
  - [2] K. Kawasaki and T. Ohta, *Physica A: Statistical Mechanics and its Applications* **116**, 573 (1982).
  - [3] T. Le Goff, P. Politi, and O. Pierre-Louis, *Phys. Rev. E* **90**, 032114 (2014).
  - [4] S. A. Safran, *Advances in Physics* **48**, 395 (1999).
  - [5] L. A. Peletier and W. C. Troy, *Spatial patterns: higher order models in physics and mechanics* (Springer, 2001).
  - [6] M. Zaks, A. Podolny, A. Nepomnyashchy, and A. Golovin, *SIAM Journal on Applied Mathematics* **66**, 700 (2005).
  - [7] P. Politi, *Phys. Rev. E* **58**, 281 (1998).
  - [8] T. Kawakatsu and T. Munakata, *Progress of Theoretical Physics* **74**, 11 (1985), <http://ptp.oxfordjournals.org/content/74/1/11.full.pdf>
  - [9] T. Nagai and K. Kawasaki, *Physica A: Statistical Mechanics and its Applications* **120**, 587 (1983).
  - [10] K. Kawasaki and T. Nagai, *Physica A: Statistical Mechanics and its Applications* **121**, 175 (1983).
  - [11] T. Nagai and K. Kawasaki, *Physica A: Statistical Mechanics and its Applications* **134**, 483 (1986).
  - [12] S.-I. Ei and T. Ohta, *Phys. Rev. E* **50**, 4672 (1994).
  - [13] J. Carr and R. L. Pego, *Communications on Pure and Applied Mathematics* **42**, 523 (1989).
  - [14] T. Le Goff, P. Politi, and O. Pierre-Louis, "Transition to coarsening for confined one-dimensional membranes," (2015), preprint.